Solar wind and geomagnetic activity influence on the equatorial plasma mass density at geosynchronous orbit

Victoir Veibell* R.S. Weigel†

June 14, 2016

Abstract

In this work we consider two types of events, determined by decreases in D_{st} below a threshold value or increases in the ρ_{eq} above a threshold value on 1-hour and 1-day time scales using the **?** dataset. From the D_{st} events, we find that there is no statistically significant relationship between either solar wind or geomagnetic activity under conditions of strong geomagnetic activity when hourly or daily averages of ρ_{eq} are considered. Although very large geomagnetic storms have been observed to correspond to large increases in the plasma trough mass density, in general ρ_{eq} following the onset of a geomagnetic storm does not depend on the storm intensity or the solar wind parameters B_z and P_{dyn}. From the ρ_{eq} events, we find a weak dependence on B_z after the onset of an event, with higher average B_z six hours after the event onset corresponding to larger ρ_{eq} events.

1 Introduction

The plasma trough is a transition region between the higher density and lower temperature plasmasphere and the lower density and higher energy magnetosphere [Mayr and Volland, 1968]. Inside of the plasmapause, the density is primarily due to ionospheric photoionization; outside of the plasmapause, the density has contributions from the co-rotating plasmasphere and Earthward convecting magnetosphere plasmas.

The dependence of the plasmapause location on geomagnetic activity was observed as early as **?**. There are well–validated models of the plasmapause boundary, as a function of L, MLT, and geomagnetic activity (Lemaire [1998], Moldwin et al. [2002], O'Brien and Moldwin [2003]). Models also exist for the plasmasphere density (Gallagher et al. [1988]; Lemaire [1998]).

The dependence of the plasma trough density on geomagnetic and solar wind conditions has not been extensively studied until the past decade (Takahashi et al. [2006]; Takahashi et al. [2010]; **?**). Earlier works that considered profiles of electron number density found a significant dependence on the plasmasphere boundary on geomagnetic activity (**?**; **?**), but there the relationship between geomagnetic activity and density in the plasma trough was not explicitly considered.

Takahashi et al. [2006] estimated magnetospheric mass density using measurements from the CRRES satellite during a 73-day period in 1991 (observations were made when CRRESS was in an elliptical, near equatorial orbit and primarily in the plasma trough region). They found that the average ion mass, $M = \rho/n_e$, had some correlation with geomagnetic activity, with more negative hourly D_{st} values corresponding to higher M and 1.5- and 3-day averages of K_p corresponding to higher M (3-hour averages of K_p had little visual correlation with M). The mass density estimates were obtained from CRRES observations in the MLT range of 12:00 and 18:00 with most observations having L between 5 and 7 R_E.

Denton et al. [2006] found a weak relationship between D_{st} and and K_p and the field line distribution of ρ using observations of the first three toroidal Alfvén harmonic frequencies for L in the range of 6-8R_E. A more pronounced peak in the distribution along a filed line near the equator was found for lower

*vveibell@gmu.edu
†rweigel@gmu.edu

D_{st} and larger K_p. The equatorial value of ρ appeared identical for the bins of D_{st} (-142 to -31 nT and -31 to 37 nT) and K_p (1.5 to 3.4 and 3.4 to 5.9) considered .

Takahashi et al. [2010] developed a mass density dataset using measurements from the Space Environment Monitor instruments on the Geostationary Operational Environmental Satellites (GOES) satellites from 1980 through 1992, with most measurements in the range of $L = 6.8 \pm 0.2 R_E$. The mass density ρ was estimated using the the Alfvén wave velocity relationship, $V_A = B/\sqrt{\mu_0 \rho}$ a magnetic field model, and a numerical solution to a wave equation with an ionospheric boundary and the assumption of a zero resistance ionosphere. The equatorial mass density, ρ_{eq}, was derived from the estimated mass density using a power law dependence on the geocentric distance to the field line of the observation, R, $\rho = \rho_{eq} L/(R/R_E)$. They found a high correlation (~ 0.93) between 27-day averages of F10.7 and 27-day medians of ρ_{eq}.

Takahashi et al. [2010] noted that downward spikes in the D_{st} index coincided with with significant changes in ρ_{eq} for L near 6.8 R_E. For five storms, two had ρ_{eq} spikes after the D_{st} drop, two had ρ_{eq} spikes before the drop, and one showed little change in ρ_{eq}. A key result was that when daily-averaged measurements were considered, an enhancement in ρ_{eq} appeared on the same day as minimum D_{st}.

Yao et al. [2008] studied the relationship between D_{st} and the number density of low-energy O^+ in different regions (ring current and plasma sheet) using the TEAMS and ESA instruments on the low-altitude and high-inclination orbiting FAST satellite and found that the average N_{O^+} across the sampled L-shells (2-14) had a strong correlation (0.88) with the minimum D_{st} of the storm. Although the correlation in the plasma trough was not calculated, the data presented for four events show that the variations in N_{O^+} tended to appear near D_{st} minimum ($\pm$ 2 hours).

? ...

The results in the papers discussed indicate that (1) the mass density in the plasma trough region is best correlated with $F10.7$ and (2) there exists a much weaker relationship between mass density and the geomagnetic activity indices K_p and D_{st}. In this work we consider the dependence of mass density estimates in the Takahashi et al. [2010] and attempt to identify and statistically characterize the relationship between geomagnetic activity with mass density in the plasma trough region. In addition, we attempt to identify solar wind processes that may drive changes in mass density.

There are several issues that are addressed in detail: (1) the plasma density measurements are sparse, (2) The plasma trough density has a high correlation with F10.7, and geomagnetic and solar wind parameters also correlate with F10.7, (3) the dependence of mass density on the north/south component of the solar wind magnetic field is expected to be nonlinear. For northward IMF, corresponding to low solar wind driving of the magnetosphere, the plasmasphere can expand past geosynchronous orbit where trough estimates of mass density are made resulting in an increase in observed density that are not due to solar wind driving; for southward IMF, events studies have shown an increase in mass density associated with strong southward IMF and enhanced magnetospheric activity (Takahashi et al. [2010]; Yao et al. [2008]).

Issue (1) is addressed by considering in detail the number of observations that are used in epoch averages around the time of two types of events, decreases in D_{st} below a threshold, and increases in ρ_{eq} above a threshold. Issue (2) is addressed using various methods to remove or isolate the F10.7 dependence. Issue (3) is addressed by considering epochs and linear correlations independent of the direction of the IMF along with separation of the epoch averages based on the northward and southward IMF.

In addition, we consider the influence of time averaging by comparing results using daily means and medians and hourly means and medians of solar wind and magnetospheric parameters.

2 Data Preparation and Overview

The parameters ρ_{eq} and $F_{10.7}$ used in this work are from the dataset of Denton [2007], which was used in Takahashi et al. [2010]; data are available from 1980 through 1991 from GOES 2,3,5, 6 and 7. All other parameters used are from Kondrashov et al. [2014] from 1972 through 2013, which are on a 1–hour time grid. ρ_{eq} is the inferred equatorial mass density based on the 3rd harmonic torodial frequency of magnetic field measurements as described in Takahashi et al. [2010]. The smallest cadence for ρ_{eq} values is 10 minutes. To compute an hourly median over the same

interval for which the solar wind parameters were averaged, the median of all ρ_{eq} values in a given hour window was used. Fill (NaN) values were used for hours in which no measurements were available. In cases where ρ_{eq} was available from multiple GOES satellites at the same time, the value from GOES 6 was selected. In the dataset, measurements from GOES 6 had the longest time span of coverage. An overview of the data used is shown in Figure 1.

In this work, events are defined to occur when D_{st} or ρ_{eq} crosses a threshold value, as indicated by horizontal dashed lines in their respective panels of Figure 1.

Figure 2 shows the long-term trends of $log(\rho_{eq})$ from GOES 6 and $F_{10.7}$ computed using the median values in 27-day non-overlapping windows. A scatter plot of these two lines is shown in the lower panel of Figure 2. The linear correlation for GOES 6 using all measurements is found to be 0.94, which is the same value documented by Takahashi et al. [2010] who used measurements from all satellites in the time interval of 1980 through 1991 using the constraint $0600 \leq MLT \leq 1200$, $K_{p3d} \geq 1.0$ and $D_{st} \geq -50$ nT. Our 27-day correlations for GOES 2, 5, and 7 are 0.81, 0.78, and 0.87, and the time range of coverage of measurements from these satellites are 1980-01-01/1983-05-16, 1983-01-01/1987-02-28, and 1983-05-27/1991-08-29 respectively.

3 Epoch Average Results

Two types of events are considered. The first is a drop in the D_{st} index **Cite Kyoto** below the threshold of -50 nT. These types of events are considered in order to determine if there is a well-defined ρ_{eq} dependence on geomagnetic activity/storms as indicated by D_{st} index. It is expected that the plasmasphere will exhibit two responses near these threshold crossings. First is the movement of the plasmasphere earthward (Lemaire [1998]) and the second is a possible change in density due to magnetospheric processes.

The second type of event is an increase in ρ_{eq} above a threshold of 20 amu/cm^3. It is expected that these increases will typically occur after period of quiet geomagnetic activity. In this case, the plasmapause boundary may move outward past geosynchronous orbit and the increase will be due to measurements being made inside the plasmapause. A second possible reason for the increase could be due to magnetospheric processes.

3.1 D_{st} Events

Our first analysis uses data only from the time interval 1989-1991, which corresponds with the interval used in the analysis in Takahashi et al. [2010]. In this interval, there were 329 D_{st} events and 70 ρ_{eq} events. For both types of events, the hour of the threshold crossing defines the zero epoch time, and for each event, $4 \cdot 24$ hours were considered before each event and $8 \cdot 24$ hours after each event. To compute the epoch averages on a daily time scale, the median value of all available measurements for all events centered on a window of ± 12 hours of the epoch zero hour was computed, and these averaging windows were shifted in increments of 24 hours. Similar results are obtained if we first reduce each event time series to have a 1-day cadence by computing medians in 1-day bins and then compute the medians across events. Error bars for each parameter are the standard deviation of the values used in computing the median divided by the square root of the number of values used.

The stack plot in the upper panel of Figure 3 shows the epoch averages for these events. The minimum D_{st} median is -48 nT. Consistent with Takahashi et al. [2010], D_{st} events correspond to elevated ρ_{eq}, although the magnitude of increase observed here is 1.5 amu/cm^3 (from 18 to 19.5 amu/cm^3) instead of the increase of ~ 10 amu/cm^3 found in Figure 11 of Takahashi et al. [2010]. The vertical green bars in the ρ_{eq} plot show the number of ρ_{eq} values that were used to compute the medians and error bars. For the non-ρ_{eq} medians, the number of measurements used in computing the medians is typically equal to the number of events, which is much larger than the number of ρ_{eq} values as we used all available measurements instead of restricting to only values where a non–fill ρ_{eq} value existed.

In the lower panel of Figure 3 it is shown that the trends seen in the analysis of 1989-1991 also hold for the entire span of measurements from GOES 6, which spans 1983-1991 - a small elevation on the day of the event relative to the day before and day after, with median averages after the day of the event being slightly lower than that before. To determine if the magnitude of the density medians in the top panel of 3 on days -1, 0, and 1 are statistically different from each other, we used a two-population bootstrap test. A bootstrap median was created by sampling the values used to compute the median on each day with replacement. The observed difference between the medians is shown in the table along with the fraction of observations in 1000 bootstrap differences with a different sign than that observed. The results are

Days	Diff(medians)	%	p-val
-1 0	-0.64	28.90% ≥ 0	0.23
-1 1	0.99	21.70% ≤ 0	0.86
1 0	-1.63	12.50% ≥ 0	0.16

Table 1: Results of test on of means of ρ_{eq} shown in the top panel of Figure 3 between days of threshold crossing near (day = 1 or -1) or on the day of a D_{st} event (day = 0).

shown in the fourth column of Table 1. The fourth column shows the results of a 2-population t-test and the fifth column indicates ???.

If a statistically significant difference in the medians between two days existed, the fraction is expected to be much smaller ($< 5\%$). In terms of a hypothesis test, we cannot reject the null hypothesis that the medians are the same with a confidence higher than 100 minus the % value shown in the table; the highest confidence level of 87.6% is in the difference between day 0 and day 1.

These tests indicate that there is not a statistically significant change in medians of ρ_{eq} on the day before and day after a threshold crossing in D_{st}. In addition, the observed differences are on the order of only 10% of the ρ_{eq}, which is small compared to the variance in the observations.

Because the dynamics of the magnetopshere take place on a time scale of less than one day, we have also considered hourly averages as shown in the top panel of Fig. 4. A total of 668 events were found in the interval of May 1983 through August 1991 with an average duration of 9 hours and a median duration of 3 hours. The error bars were computed in the same way as Fig. 3. In this plot, the overall trend is similar to that found in the bottom panel of Fig. 4 - ρ_{eq} is slightly elevated at the time of the threshold crossing of D_{st} with respect to the values one day before and after, but the elevation is small and in general not statistically significant. At this timescale no obvious change in mass density at hourly timescale is visible. This points to an issue with only looking at long-timescale trends between density and D_{st}, and allows for the possibility that other factors are influencing the long term correlation because there is no obvious connection on a short timescale. One possibility is that, as suggested in Takahashi et al. [2010], $F_{10.7}$ plays a significant role in driving long term density values which biases the long-term correlation of density and D_{st}.

The bottom panel of Fig. 4 contains the events shown in the top panel under the constraint that D_{st} remained below -50 nT for at least twelve hours after the event onset time. In the time period of elevated mass density within 12 hours of the start of the event, there were an average of **X** samples per hourly interval. This result is consistent with previous observations of large mass density spikes in the plasma trough region during large geomagnetic storms (Yao et al. [2008]; Takahashi et al. [2010] and the observation that solar wind parameters have very little correlation independent of $F_{10.7}$ (**?**). To determine of this relationship can be observed in the events of the top panel of Fig. 4, we sorted the events by the average D_{st} values in the time interval of 0-12 hours, split the events in two and recomputed the epoch averages of ρ_{eq}. The result is that there is no statistically significant difference in the mass density epoch averages for large versus small storms. This indicates that to confirm the ρ_{eq} dependence on large geomagnetic storms would require a dataset with a much larger number of strong geomagnetic storms.

3.2 ρ_{eq} Events

An alternative type of event can be defined that corresponds to large increases in ρ . Figure 5 shows the epoch time series for events in which an increase of ρ_{eq} above 20 amu/cm^2 defines the start of the event. In finding ρ_{eq} events, all fill values were replaced with linearly interpolated values. **Not including ρ_{eq} events?**

Here we see that such events tend to be associated with positive B_z^{IMF} and low geomagnetic activity (**?**).

To determine if the sign of B_z^{IMF} influences the ρ epoch time series, we separated the events by the average of B_z^{IMF} in a time window of 4 hours.

Figure (a) shows the epoch curves for $B_z^{IMF} \geq = 0$ (257) events and $B_z^{IMF} \geq = 0$ (139) have no statistically significant difference.

3.3 Conclusions

References

R. Denton. Database of Input Parameters for Tsyganenko Magnetic Field Models, 2007. URL http://www.dartmouth.edu/~rdenton/magpar/index.html.

R. E. Denton, K. Takahashi, I. A. Galkin, P. A. Nsumei, X. Huang, B. W. Reinisch, R. R. Anderson, M. K. Sleeper, and W. J. Hughes. Distribution of density along magnetospheric field lines. *Journal of Geophysical Research (Space Physics)*, 111:A04213, April 2006. doi:10.1029/2005JA011414.

D. L. Gallagher, P. D. Craven, and R. H. Comfort. An empirical model of the earth's plasmasphere. *Advances in Space Research*, 8:15–21, 1988. doi:10.1016/0273-1177(88)90258-X.

D. Kondrashov, R. Denton, Y. Y. Shprits, and H. J. Singer. Reconstruction of gaps in the past history of solar wind parameters. *Geophysical Research Letters*, 41:2702–2707, April 2014. doi:10.1002/2014GL059741.

J Lemaire. *The Earth's Plasmasphere*. Cambridge University Press, Cambridge, U.K. New York, 1998. ISBN 9780521430913.

H. G. Mayr and H. Volland. Model of magnetospheric temperature distribution. J. Geophys. Res., 73:4851–4858, August 1968. doi:10.1029/JA073i015p04851.

M. B. Moldwin, L. Downward, H. K. Rassoul, R. Amin, and R. R. Anderson. A new model of the location of the plasmapause: CRRES results. *Journal of Geophysical Research (Space Physics)*, 107:1339, November 2002. doi:10.1029/2001JA009211.

T. P. O'Brien and M. B. Moldwin. Empirical plasmapause models from magnetic indices. Geophys. Res. Lett., 30:1152, February 2003. doi:10.1029/2002GL016007.

K. Takahashi, R. E. Denton, R. R. Anderson, and W. J. Hughes. Mass density inferred from toroidal wave frequencies and its comparison to electron density. *Journal of Geophysical Research (Space Physics)*, 111:A01201, January 2006. doi:10.1029/2005JA011286.

K. Takahashi, R. E. Denton, and H. J. Singer. Solar cycle variation of geosynchronous plasma mass density derived from the frequency of standing Alfvén waves. *Journal of Geophysical Research (Space Physics)*, 115:A07207, July 2010. doi:10.1029/2009JA015243.

Y. Yao, K. Seki, Y. Miyoshi, J. P. McFadden, E. J. Lund, and C. W. Carlson. Effect of solar wind variation on low-energy O+ populations in the magnetosphere during geomagnetic storms: FAST observations. *Journal of Geophysical Research (Space Physics)*, 113, 2008. doi:10.1029/2007JA012681.

4 Figures

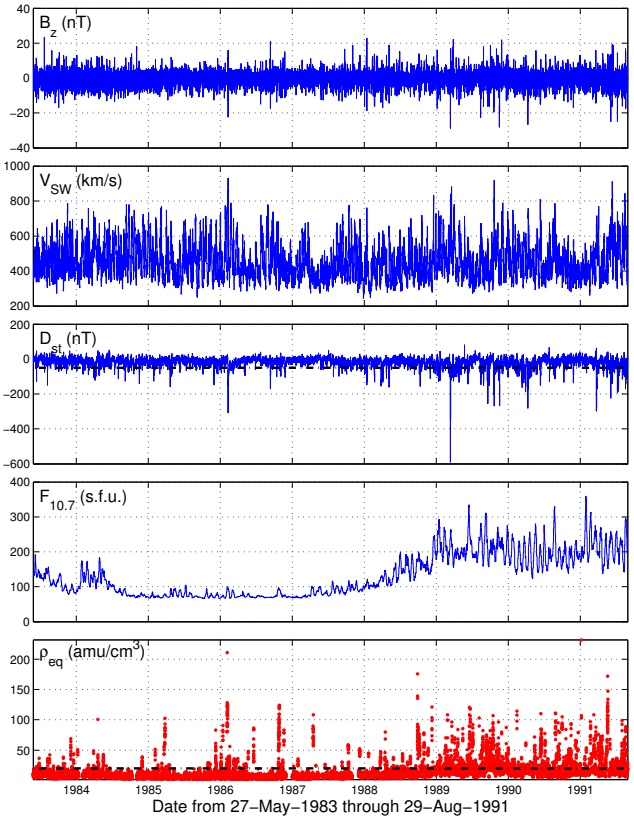

Figure 1: Overview of data used in this article. The top four panels show parameters from Kondrashov et al. [2014] and the bottom panel contains ρ_{eq} based on GOES 6 measurements from Denton [2007] after interpolation and averaging described in the text. Dashed horizontal lines in the D_{st} and ρ_{eq} panels indicate sample event cutoff thresholds of $D_{st} = -50$ nT and $\rho_{eq} = 20$ amu/cm^3 considered in Section 3.

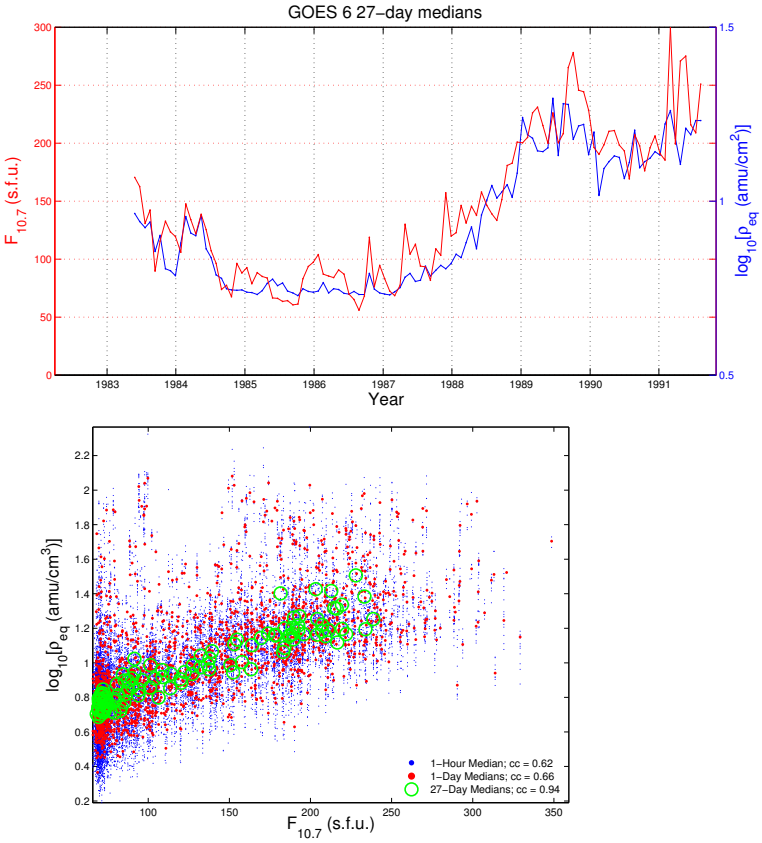

Figure 2: Top: 27-day non-overlapping medians of $F_{10.7}$ and $\log(\rho_{eq})$ from GOES 6. Bottom: Correlation between $\log(\rho_{eq})$ and $F_{10.7}$ using medians in non-overlapping hour, day, and 27-day windows.

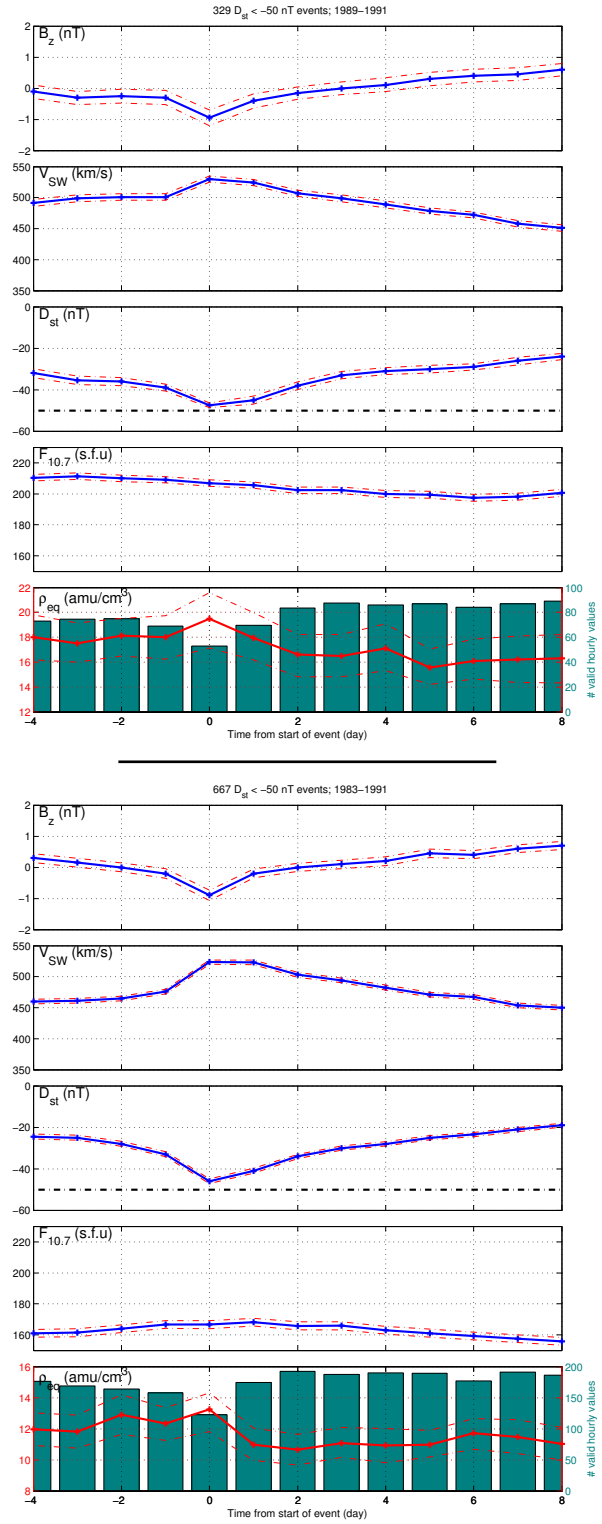

Figure 3: D_{st} events from GOES 6 using daily medians. Top: Events in the interval 1989-1991; compare to Takahashi et al. [2010] Fig. 11. Bottom: Events in the interval 1983-1991.

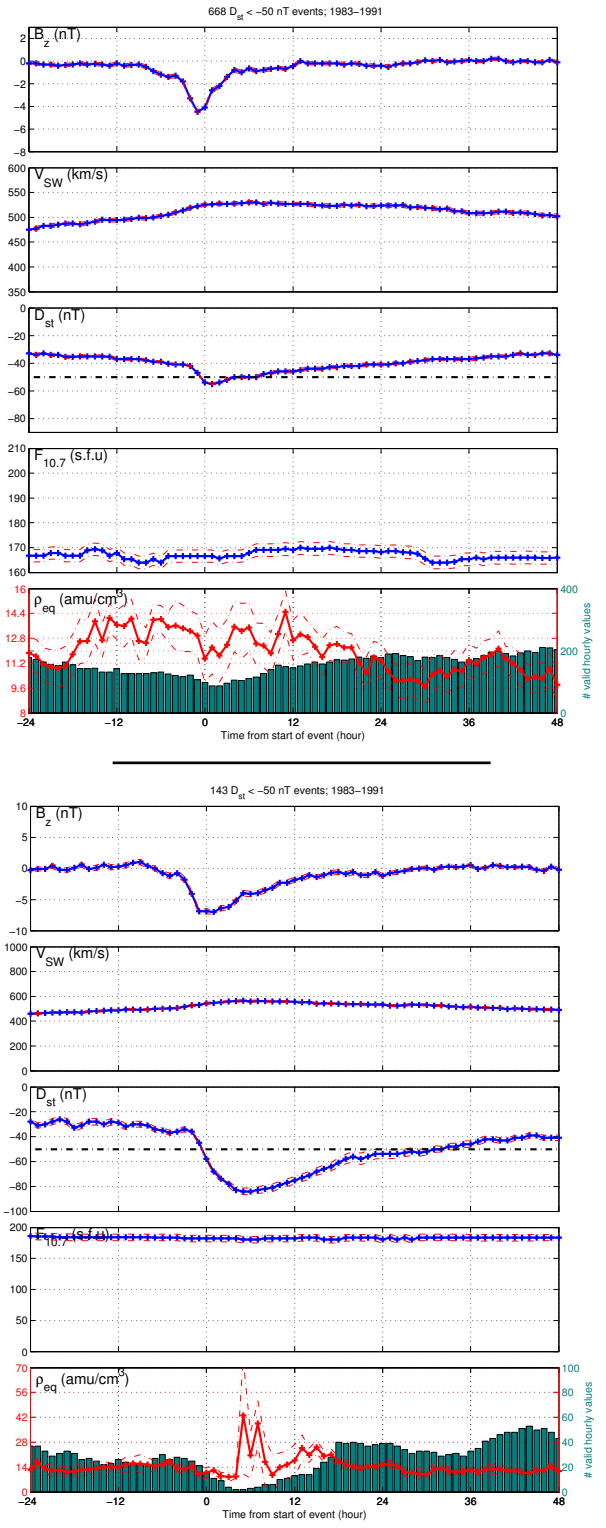

Figure 4: D_{st} events from GOES 6 using hourly medians. Top: Events in the interval 1983-1991; compare to bottom panel Fig. 3. Bottom: Same as Top except for constraint that D_{st} stayed below -50 nT for at least 12 hours after crossing below -50 nT.

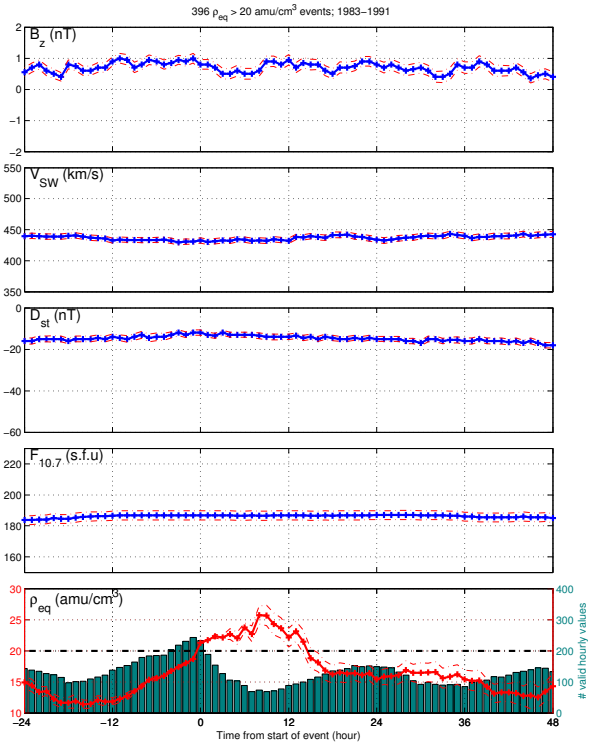

Figure 5: $\rho_{eq} > 20$ amu/cm^3 events from GOES 6 using hourly medians. As described in the text, there is no statistically significant dependence of the ρ_{eq} plot on B_z in the time interval of ± 2 hours around the event.

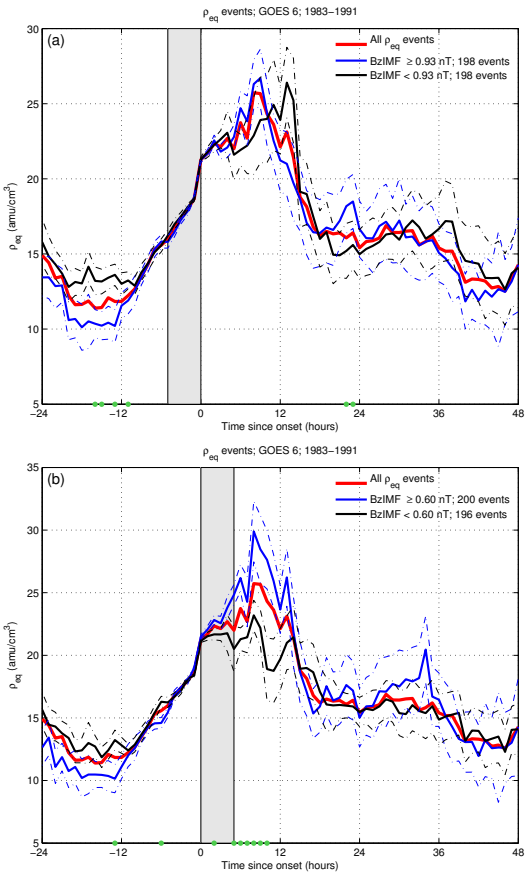

Figure 6: Binning ρ_{eq} events by B_z value (a) at onset and four hours before, and (b) at onset and four hours after.